Florida A&M University – Florida State University
College of Engineering
Gang Chen, Ph.D.
Department of Civil & Environmental Engineering
2525 Pottsdamer Street, Tallahassee, FL 32310-6046
Tel (850) 410-6303 Fax (850) 410-6142
E-mail: gchen@eng.fsu.edu

S. Typhimurium and *E. coli* O157:H7 Transport Modeling for Agricultural Practices

Annual Report

(July 1, 2007 to June 30, 2008)

Submitted to

National Research Initiative of the USDA Cooperative State Research, Education and Extension Service

by

Gang Chen and Amy Chan Hilton
Department of Civil and Environmental Engineering
FAMU-FSU College of Engineering

TABLE OF CONTENTS

LIST OF TABLES

LIST OF FIGURES

Summary

Animal waste is a valuable resource, which, when managed properly, can reduce the need for commercial fertilizer. It can also improve the soil water holding capacity and tilth. Similarly, as a new recognized water resource, nutrient-rich reclaimed wastewater supplies not only water, but also plant nutrients (especially nitrogen and phosphorus) that can benefit agricultural production. When animal waste or reclaimed wastewater is used for land applications or agricultural irrigation, the major concern is the possible spreading of infectious agents or pathogenic organisms in the soil and the subsequent possibility of groundwater contamination once the infectious agents or pathogenic organisms pass through the vadose zone and reach the groundwater table. For this research, we use *S. Typhimurium* and *E. coli* O157:H7 as model pathogenic bacteria to investigate the impact of physiological growth stage and macro nutrient ratio on bacterial surface properties and transport in the subsurface soil.

From July 2007 through June 2008, the following major tasks were accomplished: (1) *E. coli* surface property characterization under different physiological stage and macro nutrient ratio conditions, (2) effect of lipopolysaccharide extraction on bacterial transport, and (3) *lux* gene impact evaluation. Among these accomplished tasks, *E. coli* surface property characterization under different physiological stage and macro nutrient ratio conditions is the major focus. For this part of research, we demonstrated that bacteria had different surface properties under different physiological stage and macro nutrient ratio conditions. We used *E. coli* HB101 as a model strain during this research period to avoid the exposure to *S. Typhimurium* and *E. coli* O157:H7 and obtained positive results. We will repeat the same procedure for *S. Typhimurium* and *E. coli* O157:H7 for the following research period. During this research period, we also investigated the effect of lipopolysaccharide extraction on bacterial transport, which provided a possible practical means for animal waste land applications. Finally, the effect of *lux* gene insertion on bacterial surface properties was explored. This information or knowledge is needed for the following research of transport of *lux* gene-marked *S. Typhimurium* and *E. coli* O157:H7 in the subsurface soil. We have obtained positive results on *lux* gene insertion impact evaluation. We will repeat the same technology to *S. Typhimurium* and *E. coli* O157:H7 for the following research.

1. Introduction

1.1 Motivation

Animal waste should be considered a valuable resource, which, when managed properly, can reduce the need for commercial fertilizer. Animal waste can add organic matter to improve the soil water holding capacity and tilth. It also provides an economical source of nitrogen, phosphous and potassium as well as other nutrients needed for plant growth. Historically, manure generated by livestock has been practiced for land applications to improve soil tilth and fertility. Currently, it is well recognized that land applications are the best method of utilizing animal manure. In the mean time, increasing water demands owing to the growth of urbanized populations have led to constraints on existing surface and groundwater supplies. As a new recognized water resource, a wide variety of options have been developed to reuse reclaimed wastewater, among which agricultural irrigation is most commonly practiced (10). There are environmental economical benefits for reclaimed wastewater to be used for irrigation: in addition to reducing the demands on potable sources of freshwater, reuse of reclaimed wastewater for agricultural irrigation can diminish the volume of treated wastewater to be discharged directly to natural water resources of streams, rivers or lakes, resulting in a beneficial impact on the aquatic environment. Furthermore, nutrient-rich wastewater supplies not only water, but also plant nutrients (especially nitrogen and phosphorus) that can benefit agricultural production.

Both animal waste and reclaimed wastewater are rich in infectious agents or pathogenic organisms, which include viruses, bacteria and pathogenic protozoa. The majority of these pathogens are enteric in origin which can cause waterborne diseases such as salmonellosis, typhoid fever, and cholera (by bacteria); viral gastroenteritis and hepatitis A (by viruses); and amoebic dysentery and cryptosporidiosis (by protozoa) through the fecal-oral route. Bacteria are the most common pathogenic microorganisms found in animal waste and reclaimed wastewater, among which *Salmonellae*, *Shigellae*, diarrheagenic *Escherichia coli* (including *E. coli* O157:H7), *Campylobacter* and *Vibrios* are of particular concern. Viruses are also important and are potentially more infectious than bacteria. Whereas, viruses are obligate intracellular parasites and are incapable of replication outside of host organisms, which are, in most cases, bacteria. Common protozoa found in animal waste and reclaimed wastewater are *Giardia* and *Cryptosporidium*, which are relatively large pathogenic microorganisms that can multiply only in

the gastrointestinal tract of humans and other animals. They cannot multiply in the environment, but they can survive longer in water than intestinal bacteria and are more infectious and resistant to disinfection than most other microorganisms. Usually, the presence of *E. coli* is an indication that *Giardia* and *Cryptosporidium* could also be present. Thus, infectious agents or pathogenic organisms in the soil should be able to be symbolized by pathogenic bacteria. When animal waste or reclaimed wastewater is used for land applications or agricultural irrigation, the major concern is the possible spreading of infectious agents or pathogenic organisms in the soil and the possibility of groundwater contamination once the infectious agents or pathogenic organisms pass through the vadose zone and reach the groundwater table. Special care must be taken to monitor the fate and transport of these infectious agents or pathogenic organisms during animal waste land applications or agricultural irrigation using reclaimed wastewater.

Transport of the pathogenic bacteria in the soil is usually controlled by the propensity of these strains to adhere to porous media surfaces, resulting from their interactions with the surrounding environment (30). It has been demonstrated that the adhesions of pathogenic bacteria in porous media surfaces in the subsurface soil is correlated with bacterial interactions with the surrounding environment, which are determined by the pathogenic bacterial cell outer membrane composition in terms of proteins, lipopolysaccharides and phospholipids, etc. (4, 6, 14, 27). Recently, researchers discovered that pathogenic bacteria exhibited different outer membrane composition resulting from physiological and metabolic changes during the growth cycle (1). Therefore, pathogenic bacterial physiological growth stage should play an important role in pathogenic bacterial adhesion and transport in the subsurface soil. The pathogenic bacterial outer membrane composition is also impacted by the available macro nutrients of carbon and nitrogen. Practically, the pathogenic bacterial outer membrane composition can be characterized by pathogenic bacterial surface thermodynamic properties, based on which interactions between pathogenic bacteria and the surrounding environment can be quantified according to the traditional and extended Derjaguin-Landau-Verwey-Overbeek (DLVO) theory (5, 12, 28, 31).

As the fate and transport of pathogen bacteria determine the actual field practices of animal waste land applications and reclaimed wastewater agricultural irrigation, a thorough comprehension of the transport processes of pathogenic bacteria in the subsurface soil will

provide invaluable guidelines for farmers to practice animal waste and reclaimed wastewater agricultural applications.

1.2 Objectives

Our major research interest of this research period concerns the impact of pathogenic bacterial physiological growth stage and macro nutrient ratio on the fate and transport of pathogenic bacteria in the subsurface soil. We believe pathogenic bacterial transport is controlled by their interactions with the surrounding environment, which are determined by pathogenic bacterial surface thermodynamic properties. From July 2007 through June 2008, the following major tasks were accomplished: (1) *E. coli* surface property characterization under different physiological stage and macro nutrient ratio conditions, (2) effect of lipopolysaccharide extraction on bacterial transport, and (3) *lux* gene impact evaluation.

Among these accomplished tasks, *E. coli* surface property characterization under different physiological stage and macro nutrient ratio conditions is the major focus. For this part of research, we demonstrated that bacteria had different surface properties under different physiological stage and macro nutrient ratio conditions. We used *E. coli* HB101 as a model strain during this research period to avoid the exposure to *S. Typhimurium* and *E. coli* O157:H7 and obtained positive results. We will repeat the same procedure for *S. Typhimurium* and *E. coli* O157:H7 for the following research period. During this research period, we also investigated the effect of lipopolysaccharide extraction on bacterial transport, which provided a possible practical means for animal waste land applications. Finally, the effect of *lux* gene insertion on bacterial surface properties was explored. This information or knowledge is needed for the following research of transport of *lux* gene-marked *S. Typhimurium* and *E. coli* O157:H7 in the subsurface soil. We have obtained positive results on *lux* gene insertion impact evaluation. We will repeat the same technology to *S. Typhimurium* and *E. coli* O157:H7 for the following research.

2. Impact of Carbon and Nitrogen Conditions and Physiological Stage on *E. coli* Surface Thermodynamics

2.1 Material and Methods

E. coli strain used in this part of research was *E. coli* HB101, a plasmidless non-fimbriated bacterium, obtained from ATCC (33694). After inoculated with 1 ml (1.0%) stationary phase culture, *E. coli* was grown in 250 Erlenmeyer flasks containing 100 ml minimal media, consisting of 5.44 g KH_2PO_4 and 6 ml salt solution together with carbon and nitrogen sources. The salt solution is composed 10 g $MgSO_4 \cdot 7H_2O$, 1.0 g $MnCl_2 \cdot 4H_2O$, 0.4 g $FeSO_4 \cdot 7H_2O$ and 0.1 g $CaCl_2 \cdot 2H_2O$ dissolved in 1 liter distilled water. Glucose served as the carbon source and ammonia served as the nitrogen source. The combination of each of the carbon and nitrogen sources at different C/N ratios formed 3 different media formations (Table 1). Initial pH of the media was adjusted to 7.4 with 1 N HCl or 1 N NaOH. The media were sterilized by autoclaving (121^{o}C and 1 atm) for 20 min, after which glucose was filter-sterilized and aseptically added to the autoclaved minimal media. The flasks were continuously trembled at 150 rpm on a Gyrotory Water Bath (Model G76, New Brunswick Scientific Co. Inc., Edison, NJ) at 37^{o}C. Physiological stage of the bacteria was quantified through biochemical assay using ATP analysis (7). After inoculated on the Gyratory Water Bath Shaker at 37^{o}C, 50 μl of the *E. coli* culture from different media formations was sampled every 30 minutes for up to 60 hours. The light emission produced by the reaction of ATP extracted from the cells with luciferase as measured by a luminometer (TD-20/20, Turner Design, Sunnyvale, CA) was compared to an ATP standard (2.5×10^{-8} g ml^{-1} ATP which is equivalent to 5×10^{7} bacteria per ml) (10 μg ml^{-1} ATP in HEPES buffer, Turner Design, Sunnyvale, CA) to determine the viable bacterial cell numbers. Growth curves of the viable cell number versus time were thus obtained, which were used as the references for the determination of the physiological stage for *E. coli* in different media formations.

Table 1. Carbon and Nitrogen Sources in Different Media Formations

Media	C Source	N Source	C:N (g g^{-1})	Limitation
1	Glucose 0.2 g	NH_4Cl 0.06 g	5 : 1	
2	Glucose 0.2 g	NH_4Cl 0.01 g	30 : 1	N
3	Glucose 0.2 g	NH_4Cl 0.16 g	1 : 1.5	C

Surface thermodynamics of *E. coli* was measured by contact angle measurements (Contact Angle Meter, Tantec, Schaumburg, IL) following the method described by Grasso *et al*. (16). *E. coli* collected from different media formations at different physiological stage (predetermined by ATP analysis) were washed twice with nano-pure deionized water (NPDI), and then resuspended in NPDI. Bacterial suspension was then vacuum-filtered on silver metal membrane filters (0.45 μm, Osmonic, Inc.) and air-dried for about 30 minutes before the contact-angle measurements were taken. The amount of cells on the silver filter was approximately 13 mg to ensure multi-layer covering of the membrane. The moisture content was kept in the range of 25% to 30%. One apolar liquid, diiodomethane and two polar liquids, water and formamine were used for the measurements. Each measurement was repeated 30 times and the average values were fit in Young-Dupré's equation to estimate the bacterial surface thermodynamics.

$$(1+\cos\theta)\gamma_L = 2(\sqrt{\gamma_S^{LW}\gamma_L^{LW}} + \sqrt{\gamma_S^{+}\gamma_L^{-}} + \sqrt{\gamma_S^{-}\gamma_L^{+}}) \quad (1)$$

where θ is the measured contact angle (degree); γ_L is the surface tension of the liquid used for the measurements (mJ m^{-2}); γ^{LW} is the Liftshitz-van der Waals component of surface tension (subscript "S" for solid, "L" for liquid) (mJ m^{-2}); and $\gamma^{+}$and γ^{-} are the electron-acceptor and electron-donor parameter of Lewis acid/base component of the surface tension (subscript "S" for solid, "L" for liquid) (mJ m^{-2}).

ζ-potentials of the bacterial strains were measured using Lazer Zee Meter (Model 501, Pen Kem, Inc.), which was also repeated 30 times. Similar to the contact-angle measurement, bacterial strains were washed twice with NPDI and suspended in NPDI for the measurements.

Bacterial surface components were analyzed using infrared spectroscopy (IR) (Perkin-Elmer, 283B) with potassium bromide serving as the crystalline media. After NPDI washing, air-dried bacterial strains collected from different media formations at different physiological stage were mixed with potassium bromide to make crystal media before they were put into IR for the analysis. Each sample was evaluated in triplicates and the inconsistency of the peaks of relative transmission was within 5% (95% CI, t-test). The frequencies of the peaks were referred to the library of reference curves (2).

2.2 Results and Discussion

When carbon was limited (C/N = 1:1.5), the diiodomethane contact angle and formamine contact angle decreased as compared with no carbon and nitrogen limitation (C/N = 5:1) (Table 2). But there was no obvious difference with respect to water contact angle. When nitrogen was limited (C/N = 30:1), both diiodomethane contact angle, formamine contact angle and water contact angle increased as compared with no carbon and nitrogen limitation (C/N = 5: 1). There was no obvious change for diiodomethane contact angle with variations of physiological stage. For formamine contact angle and water contact angle, there was a general trend of decrease from logarithmic physiological stage to stationary physiological stage and re-bounced back at the decay physiological stage. *E. coli* had the most negative ζ-potential at the stationary physiological stage, the least at the decay physiological stage.

Table 2. Contact Angles of *E. coli* Cultured under Different Carbon and Nitrogen Conditions and Physiological Stage

C:N ($g\ g^{-1}$)	θ^D (^{o})	θ^F (^{o})	θ^W (^{o})	ζ-potential (mV)
		Logarithmic Growth Stage		
5 : 1	40.0 ± 0.6	21.1 ± 0.4	13.1 ± 0.5	-16.1 ± 0.4
30 : 1	44.3 ± 0.4	30.0 ± 0.3	18.8 ± 0.6	-17.2 ± 0.3
1 : 1.5	34.0 ± 0.7	12.2 ± 0.5	13.3 ± 0.3	-14.4 ± 0.2
		Stationary Growth Stage		
5 : 1	41.0 ± 0.3	23.6 ± 0.3	12.3 ± 0.7	-16.3 ± 0.4
30 : 1	44.5 ± 0.1	31.0 ± 0.7	17.1 ± 0.3	-17.8 ± 0.1
1 : 1.5	32.6 ± 0.6	8.81 ± 0.8	1.06 ± 0.8	-15.1 ± 0.3
		Decay Growth Stage		
5 : 1	40.0 ± 0.4	24.4 ± 0.9	15.3 ± 0.3	-16.2 ± 0.4

30 : 1	42.4 ± 0.3	31.6 ± 1.2	20.5 ± 0.9	-17.0 ± 0.5
1 : 1.5	32.2 ± 0.5	10.8 ± 0.5	8.04 ± 0.2	-13.7 ± 0.5

When carbon was limited (C/N = 1:1.5), *E. coli* had greatest γ^+ and γ^{LW}, but smallest γ^- than that when there was no substrate or nutrient limitation (Table 3). When nitrogen was the limiting factor (C/N = 30:1), *E. coli* had smallest γ^+ and γ^{LW}, but greatest γ^- than that when there was no substrate or nutrient limitation. van Oss (31) has previously suggested that the γ^{LW} values for a considerable number of biological and many other organic materials are typically equal to 40 mJ/m^2 with minor variability. This was supported by the results of this research. The γ^{LW} values of *E. coli* cultured under different carbon and nitrogen conditions at different physiological stage were within the range of 38 mJ/m^2 to 44 mJ/m^2. As γ^{LW} was obtained by using the apolar liquid of diiodomethane and *E. coli* was essentially monopolar (γ^- was two order in magnitude greater than γ^+), monopolarity was reflected by the cohesion with relatively stable γ^{LW} (31). Carbon and nitrogen conditions had obvious effect on γ^{LW}, while the effect of physiological stage on γ^{LW} was minimal (Figure 1).

Table 3. Surface Properties of *E. coli* Cultured under Different Carbon and Nitrogen Conditions and Physiological Stage

C:N ($g\ g^{-1}$)	$\gamma+$ ($mJ\ m^{-2}$)	γ^- ($mJ\ m^{-2}$)	γ^{LW} ($mJ\ m^{-2}$)
	Logarithmic		
5 : 1	0.72	57.2	39.6
30 : 1	0.47	59.2	37.4
1 : 1.5	0.79	53.4	42.5
	Stationary		
5 : 1	0.61	59.1	39.1

30 : 1	0.38	61.4	37.2
1 : 1.5	0.72	56.2	43.1
		Decay	
5 : 1	0.54	57.9	39.6
30 : 1	0.29	59.2	38.4
1 : 1.5	0.67	55.4	43.3

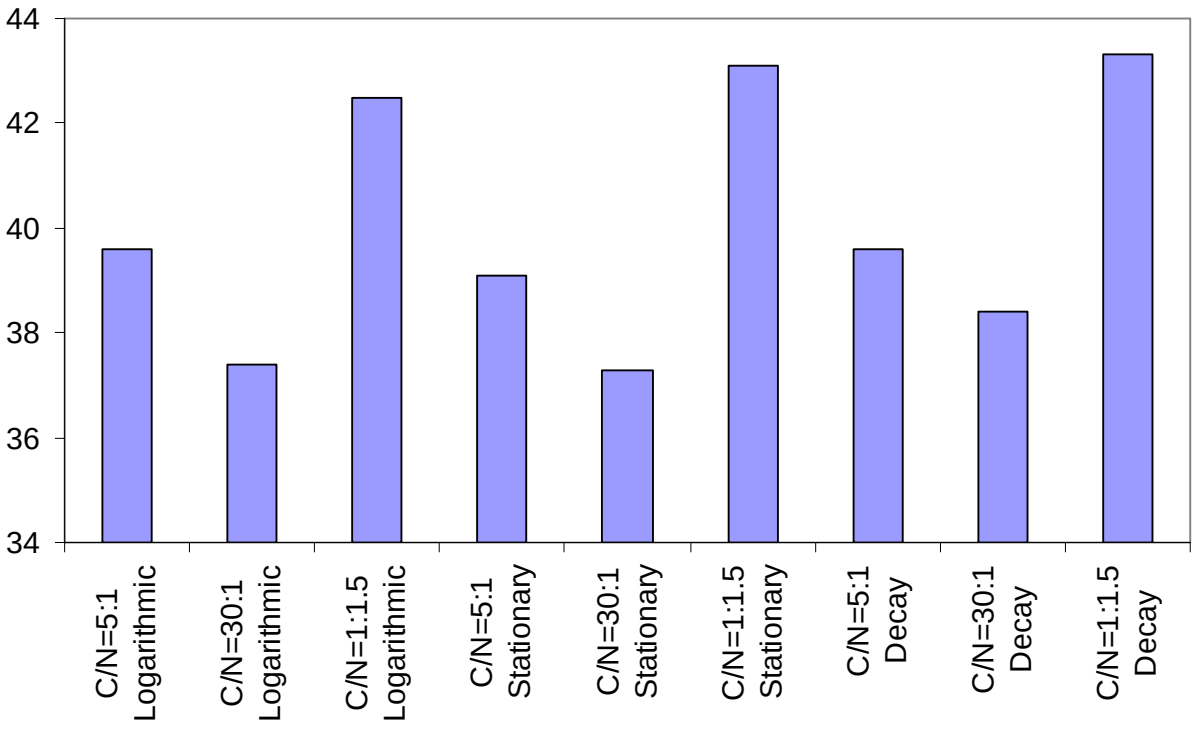

Figure 1. van der Waals Component Surface Tension

As *E. coli* was monopolar, γ^- played a more important role than γ^+ in determining the Lewis acid-base interaction with the surrounding environment. γ^- appeared primarily to be responsible for the stability of the bacterial suspension. In stationary state, γ^- value increased by 2% ~ 4% from logarithmic state (Figure 2). This suggested that the hydrophilicity of *E. coli* decreased when

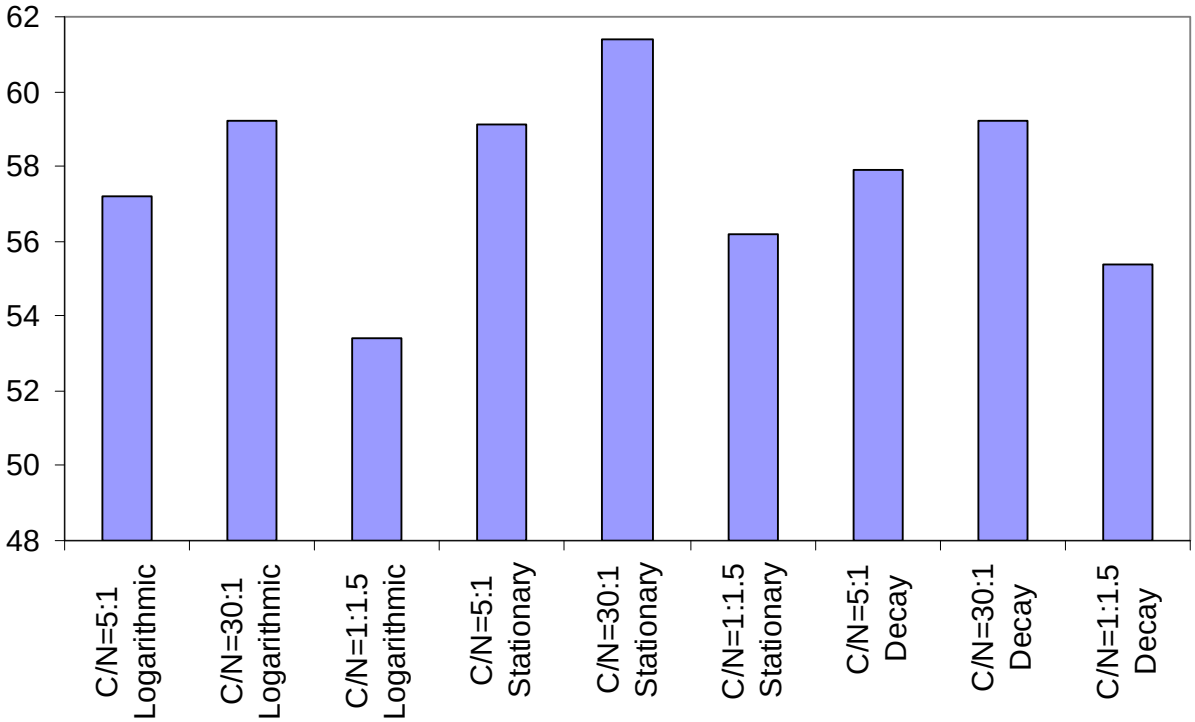

Figure 2. Electron Donor Parameter of Lewis Acid/Base Component Surface Tension

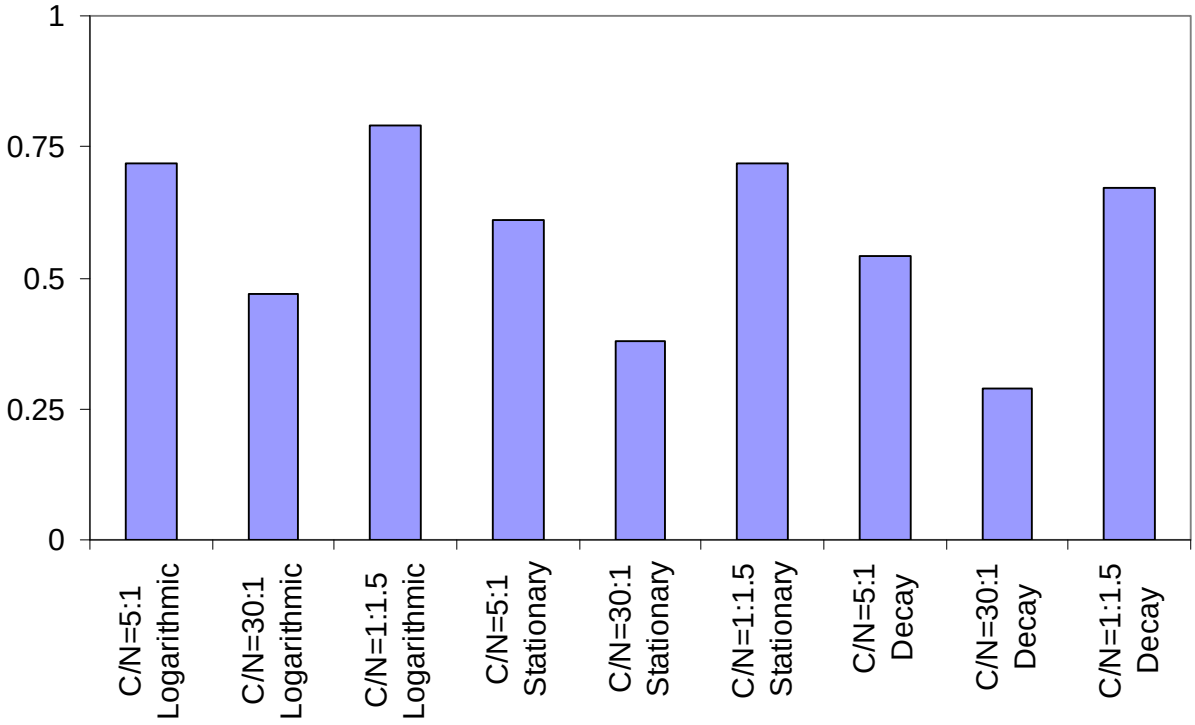

Figure 3. Electron Acceptor Parameter of Lewis Acid/Base Component Surface Tension

changing from logarithmic state to stationary state. Conversely, γ^- value decreased by 6% ~ 10% from the stationary state to decay state. γ^+ value decreased by 3% ~ 4% from logarithmic state and increased by 6% ~ 13% from stationary state to decay state (Figure 3).

To develop an explanation for this phenomenon, further investigation was performed through the study of chemical structure of the bacterial surfaces at different physiological stage. By using infrared spectroscopy (IR), the bacteria surfaces were found to be characterized by a variety of different functional groups of aldehydes (RCOH) (peaks shown at wavenumber of 1700 cm-1), ketones (RCOR) (1680 cm-1), carboxylic acids (RCOOH, RCOO-) (1690 cm^{-1}, 1600 cm^{-1}), carbonyl groups (CH3CO-) (1320 cm^{-1}), peptide bond (-CO-NH-) (1500 cm^{-1}), ethers (-CH2-O-, CH3-O-, -C-O-C-) (1000 cm^{-1}, 980 cm^{-1}, 1060 cm^{-1}), ethenyl groups (-CH=CH-, >C=CH2, -CH=CH2) (700 cm^{-1}, 830 cm^{-1}, 860 cm^{-1}), etc., as well as hydrogen (H-) (2900 cm^{-1}) and (hydroxyl) (OH-) (3600 cm^{-1}), which were due to the contribution of water.

Table 4. Relevant Transmissions of Different Functional Groups

	5:1 L*	30:1 L	1:1.5 L	5:1 S	30:1 S	1:1.5 S	5:1 D	30:1 D	1:1.5 D
RCOH	18.6	24.7	16.2	35.2	38.9	32.4	28.6	32.4	24.2
RCOR	24.5	29.4	20.3	43.2	56.1	39.2	34.6	41.1	16.7
RCOOH	N/A	18.1	N/A	N/A	20.5	N/A	N/A	20.1	N/A
$RCOO^-$	30.4	36.2	26.4	48.7	51.0	43.1	38.2	43.4	34.2
CH_3CO^-	53.7	47.2	55.2	57.6	52.4	59.4	55.6	48.2	58.1
-CO-NH-	43.1	34.1	46.2	43.4	36.1	47.6	49.4	38.5	52.4
$-CH_2-O-$	58.7	45.3	60.7	61.6	42.4	63.5	67.8	44.6	67.1
CH_3-O-	N/A	N/A	16.4	N/A	N/A	18.7	N/A	N/A	17.5
-C-O-C-	61.4	39.6	67.8	59.8	37.6	63.4	71.7	42.2	72.5
-CH=CH-	60.7	52.4	62.4	61.5	50.3	65.2	61.5	52.3	60.5
$>C=CH_2$	77.6	66.7	76.2	74.8	61.2	73.2	77.7	64.3	77.4
$-CH=CH_2$	77.1	63.5	77.2	77.7	62.7	76.4	77.2	63.7	77.1

*5:1 — Carbon/Nitrogen = 5:1, 30:1 — Carbon/Nitrogen = 30:1, 1.5:1 — Carbon/Nitrogen = 1.5:1, L — logarithmic State, S — Stationary State, D — Decay State.

E. coli had more functional groups that favored the electron-donor parameter, γ^-, (hydrogen-binding groups) such as RCOH which showed peaks at wavenumber between 1400 and 1700 cm^{-1} at stationary state than at logarithmic state and decay state (Figure 4). When cultured under C/N = 5:1, the relevant transmission of RCOH for *E. coli* increased from 18.6 to 35.2 from logarithmic state to stationary state and decreased back to 28.6 at decay state. Similar observations were made for *E. coli* cultured at C/N = 30:1 and 1.5:1 (Figure 5 and Figure 6).

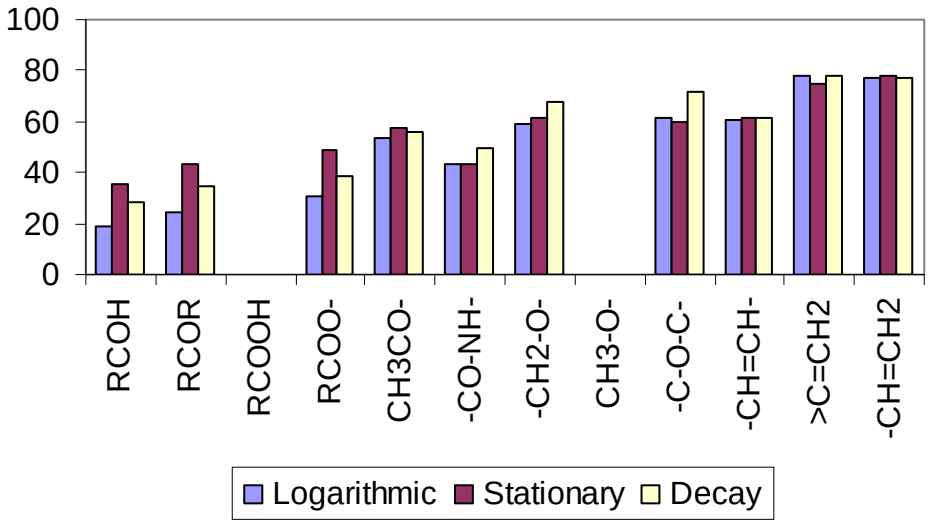

Figure 4. Relevant Transmissions of Functional Groups of *E. coli* Cultured at C/N = 5:1

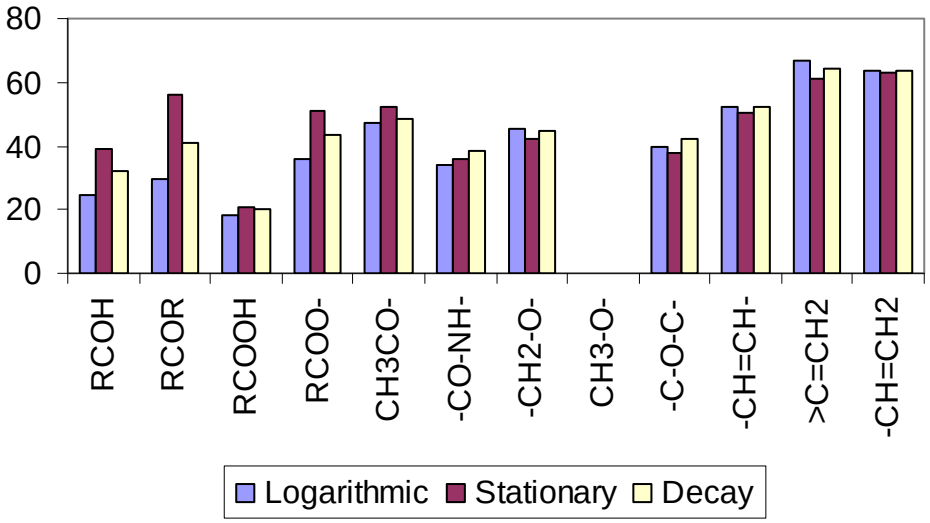

Figure 5. Relevant Transmissions of Functional Groups of *E. coli* Cultured at C/N = 30:1

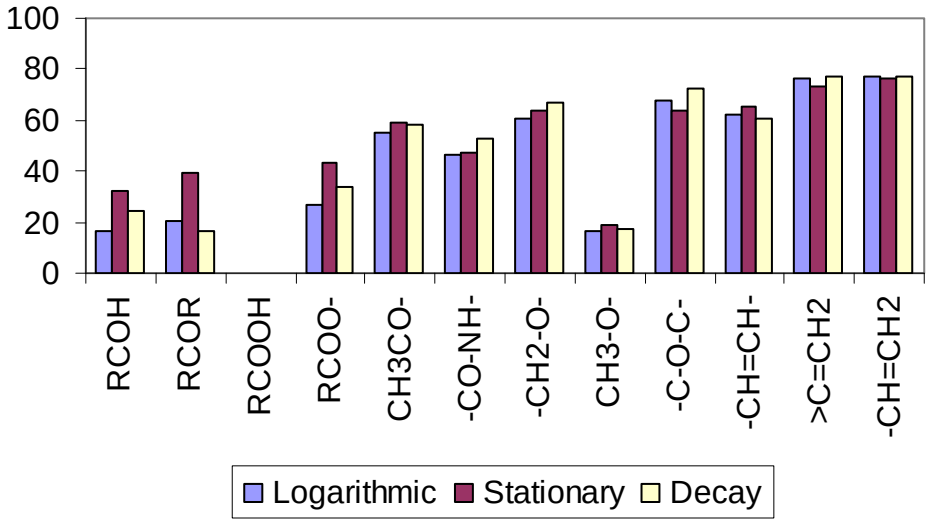

Figure 6. Relevant Transmissions of Functional Groups of *E. coli* Cultured at C/N = 1:1.5

E. coli had more functional groups that favored the electron-donor parameter, γ^-, (hydrogen-binding groups) such as RCOH and less functional groups that favored the electron-acceptor parameter, γ^+, (electron-binding groups) such as CH_3-CO- when cultured under C/N = 30:1 as compared to those cultured under C/N = 5:1 and C/N = 1.5:1 (Figure 7, Figure 8 and Figure 9). At the stationary state, the relevant transmission of RCOH for *E. coli* was 38.9 when cultured under C/N = 30:1 as compared to 35.2 and 32.4 when cultured under C/N = 5:1 and C/N = 1.5: 1 (Figure 8). Similarly, the relevant transmission of CH_3-CO- for *E. coli* was 52.4 when cultured under C/N = 30:1 as compared to 57.6 and 59.4 when cultured under C/N = 5:1 and C/N = 1.5: 1 (Figure 8). Similar observations were made for *E. coli* at logarithmic state and decay state (Figure 7 and Figure 9).

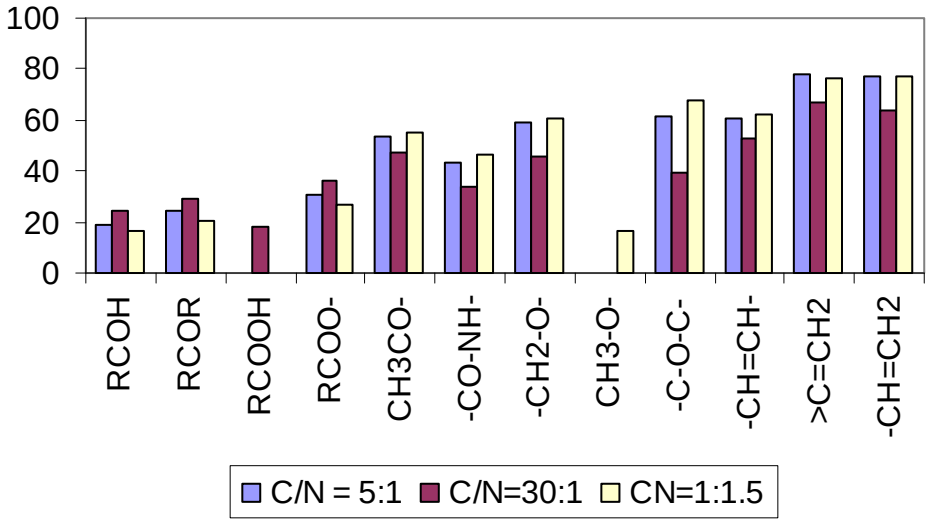

Figure 7. Relevant Transmissions of Functional Groups of *E. coli* Cultured at Logarithmic State

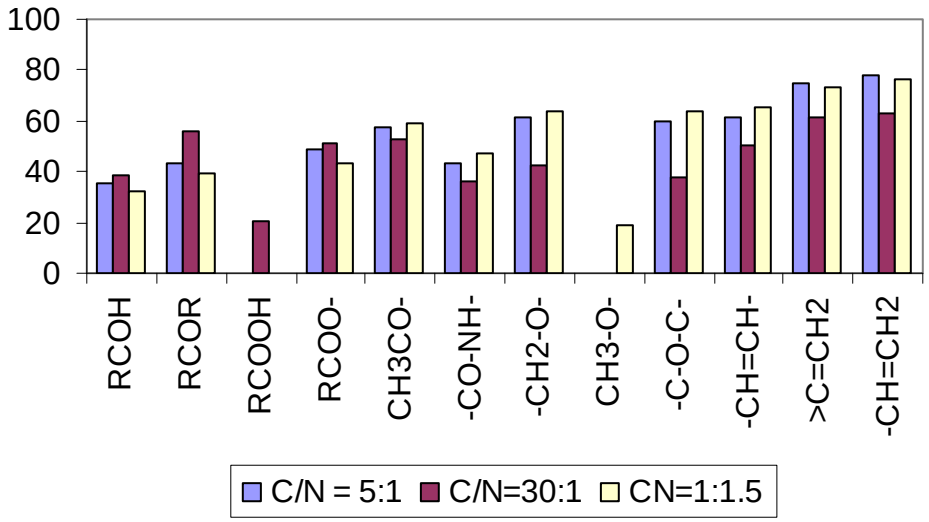

Figure 8. Relevant Transmissions of Functional Groups of *E. coli* Cultured at Stationary State

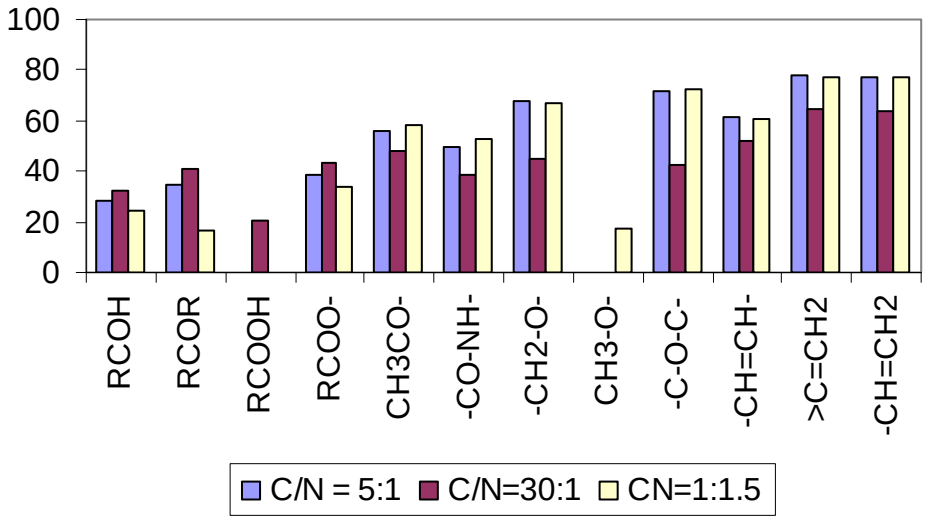

Figure 9. Relevant Transmissions of Functional Groups of *E. coli* Cultured at Decay State

3. Impact of Lipopolysaccharide Extraction on Bacterial Transport

When animal waste or reclaimed wastewater is used for land applications or agricultural irrigation, proper treatment is required either to kill the pathogens or to enhance the retention of the pathogens in the subsurface soil to protect the groundwater from being contaminated. In this study, we investigated the impact of lipopolysaccharide extraction on bacterial retention in porous media (silica sand) using column experiments. Three gram-negative bacterial strains of *Escherichia coli*, *Pseudomonas fluorescens*, and *Pseudomonas aeruginosa* were used as model bacterial strains. The transport of these three strains was described by the two-region (equilibrium/kinetic) model. After lipopolysaccharide extraction, all these three strains showed greater retention in the porous media. Increase in retention after the lipopolysaccharide extraction was most pronounced for *Pseudomonas fluorescens* and least for *E. coli*. Bacterial retention in the porous media was correlated with their interactions with the porous media.

3.1 Material and Methods

Gram-negative bacterial strains used in this research, *Escherichia coli* k12 (ATCC 29181), *Pseudomonas fluorescens* (ATCC 17559), and *Pseudomonas aeruginosa* (ATCC 15152) were cultured in minimal salt media, which had a composition of KH_2PO_4, 160 mg/l; K_2HPO_4, 420 mg/l; Na_2HPO_4, 50 mg/l; NH_4Cl, 40 mg/l; $MgSO_4 \cdot 7H_2O$, 50 mg/l; $CaCl_2$, 50 mg/l; $FeCl_3 \cdot 6H_2O$,

0.5 mg/l; $MnSO_4 \cdot 4H_2O$, 0.05 mg/l; H_3BO_3, 0.1 mg/l; $ZnSO_4 \cdot 7H_2O$, 0.05 mg/l; $(NH4)_6Mo_7O_{24}$, 0.03 mg/l; NH_4Cl, 0.6 g/l, and glucose, 2 g/l. The media were adjusted to pH 7.4 with 1 N HCl or 1 N NaOH. Before usage, the media were sterilized by autoclaving (121^{o}C and 1 atm) for 20 min. Glucose was filter-sterilized and aseptically added to the autoclaved minimal salt media. Bacterial cells collected from the stationary growth state were centrifuged at 2500 × g (Damon/IEC Divison, Needham Heights, MA) and washed twice with a sterilized phosphate-buffered saline solution (pH 7.0). The bacterial cells were then divided into two aliquots. One aliquot was re-suspended in sterilized nano-pure de-ionized water at a concentration of 5×10^8 cells/ml and used as injectants for column experiments as controls.

Lipopolysaccharide was extracted for the other aliquot following the method modified from Hancock and Poxton as described below (17). Bacterial cells were further washed and re-suspended in sterilized nano-pure de-ionized water at a concentration of 5% (W/V) and mixed with equal volume of 90% (W/W) aqueous phenol at room temperature for 15 min. The mixture was transferred to centrifuge tubes and cooled in ice until phase separation occurred. The tubes were then centrifuged at 5000 × g at 0^{o}C for 15 min. The precipitate was then washed and re-suspended in sterilized nano-pure de-ionized water at a concentration of 5×10^8 cells/ml and used as injectants for column experiments as lipopolysaccharide extracted cells.

Bacterial hydrodynamic radii were measured using a Malven Zetasizer (3000 Has, Malvern Instruments Ltd., Malvern, Worcs, UK) by suspending bacterial cells in the sterilized phosphate-buffered saline solution (pH 7.0), which were determined to be 1.0 μm, 0.30 μm, and 0.30 μm for *E. coli*, *P. fluorescens*, and *P. aeruginosa*, respectively. There was no observed variation in bacterial size after lipopolysaccharide extraction. The bacterial concentration for both control and treated bacterial strains was quantified by A_{600} measurement as compared to standard curves of *E. coli* MM294 grown in LB broth.

The porous media used in this research were silica sand (8 mesh) from Fisher Scientific (Pittsburg, PA). Silica sand was first rinsed with de-ionized water and then treated with sodium acetate, hydrogen peroxide, sodium dithionate and sodium citrate to remove organic matters. Silica sand was then extensively flushed with sterilized nano-pure de-ionized water until the

electrical conductivity was less than 1 dS/m. Before experiments, silica sand was sterilized at 121^{o}C and 1 atm for 20 min.

3.2 Column Experiments

Column experiments were conducted using an acrylic column (2.5 cm × 15, Kimble-Kontes, Vineland, NJ). The column was oriented vertically and sealed at the bottom with a custom frit to permit the flow of water and retain the media. For each column experiment, a fresh column was packed. Silica sand was packed in the column through CO_2 solvation to eliminate air pockets. Prior to starting each experiment, approximately 100 pore volumes of sterilized nano-pure de-ionized water was eluted through the column by a peristaltic pump to stabilize the column. A conservative pulse tracer (nitrate) breakthrough curve was generated separately before the introduction of bacterial suspension to estimate the porous media porosity and solute dispersion in the porous media. Based on the tracer experiments, the porosity of the porous media was determined to be 0.38. The pore size of the porous media was thus estimated to be greater than 1 mm for this research. Since the size of the bacterial strains was in the range of 0.30 μm to 1.0 μm, clogging was considered to be negligible during bacterial transport in the column.

For each run, one pore volume of bacterial suspension was pumped into the column at a flow rate of 0.56 ml/min. The column was then flushed with sterilized nano-pure de-ionized water alone for up to 50 pore volumes until no cell could be detected in the elution. Elution was collected by a fraction collector and was measured for bacterial concentration by A_{600} measurement. After each run, a breakthrough curve was generated and mass balance analysis was performed. For each column experiment, three runs were performed, and the inconsistency of breakthrough curves was within 5% (95% CI).

Model calculations with support of numerical simulation techniques have aided in the identification of the key processes that govern the bacterial transport and adsorption in the porous media, which makes it possible to evaluate bacterial adsorption mechanisms more effectively. Under saturated conditions, bacterial transport is controlled by both kinetic adsorption and equilibrium adsorption processes, which has been proven to be true for bacterial transport in sand columns (19, 25). Bacterial transport through saturated porous media can thus

be described by the equilibrium-kinetic two-region concept model based on the assumption that bacteria are deposited in the kinetic adsorption region only, where bacteria suffer from time dependent, irreversible retention (32):

$$(1+\frac{f\rho_b K_d}{\eta})\frac{\partial C}{\partial t} = D\frac{\partial^2 C}{\partial x^2} - v\frac{\partial C}{\partial x} - \frac{\alpha\rho_b}{\eta}[(1-f)K_d C - S_k] \quad (2)$$

$$\frac{\partial S_k}{\partial t} = \alpha[(1-f)K_d C - S_k] - \mu_{s,k} S_k \quad (3)$$

where C is the bacterial concentration in the aqueous phase (cells/m^3); S_k is the bacterial concentration on the kinetic adsorption sites (cells/g); t is the elapsed time (sec); f is the fraction of adsorption sites that equilibrate with the bacteria in the aqueous phase (-); ρ_b is the bulk density (g/m^3); K_d is the partitioning coefficient of bacteria to the equilibrium adsorption sites (m^3/g); η is the porosity of the porous media (m^3/m^3); D is the longitudinal dispersion coefficient (m^2/sec); x is the coordinate parallel to the flow (m); v is the pore velocity (m/sec); α is the first order mass transfer coefficient (sec^{-1}), governing the rate of bacterial exchange between equilibrium and kinetic adsorption sites; and $\mu_{s,k}$ is the first order bacterial deposition coefficient on the kinetic adsorption sites (sec^{-1}). Transport parameters in equations (1) and (2) were obtained by fitting the experimentally obtained bacterial breakthrough data using CXTFIT 2.1 (32). All these parameters were optimized by minimizing the sum of the squared differences between observed and fitted concentrations using the nonlinear least-square method.

3.3 Results and Discussion

3.3.1 Tracer Transport

Trace (NO_3^-) transport was performed before bacterial transport experiments. Nearly all the input tracer was eluted from the column. The tracer breakthrough curve was characterized by a breakthrough front and a lasting elution tail (Figure 10). The lasting tail of the tracer breakthrough curve indicated possible retardation of nitrate in the column. This may be resulted from the remaining organic content of the media. The tracer breakthrough curve was simulated with the equilibrium-kinetic two-region concept model. During the model simulation, we set the retardation factor equal to 1.0, i.e., $K_d = 0$. This was based on the consideration that nitrate should not be retarded in the media as a conservative tracer. We also set the deposition coefficient $\mu_{s,k}$ equal to zero, i.e., no retention for nitrate in the media. This is true since nearly

all the input nitrate was eluted from the column at the end of the tracer experiment. During the simulation, the velocity was fixed at 0.3 cm/min and the initial D was set as 7.89 cm^2/min. After the simulation, D was determined to be 3.35 cm^2/min, which was then used for all the simulations of bacterial transport.

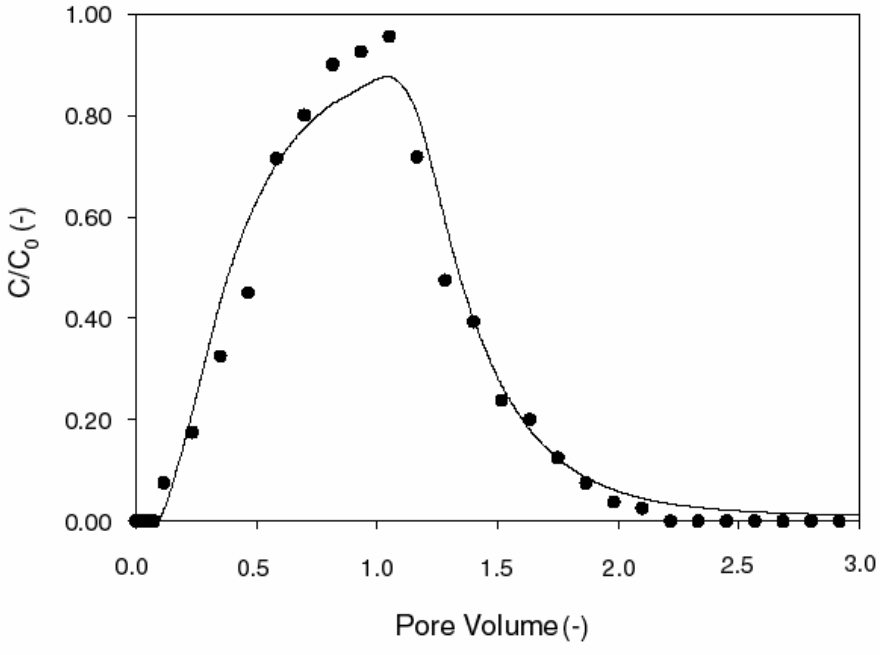

Figure 10. Nitrate Breakthrough Curves (Symbols) and Model Simulations (Lines)

3.3.2 Bacterial Transport

Under water saturated conditions, bacteria were retained in the media during transport for all the three strains with or without lipopolysaccharide extraction. Bacterial breakthrough curves displayed a narrow self-sharpening front, which became broader and diffuser at the elution limb (Figure 11). Also, the breakthrough fronts corresponded to the arrival of the infiltration at the outlet of the column. The long-lasting tails of the breakthrough curves indicated kinetic-controlled bacterial retention in the column. Among the three bacterial strains investigated in this research, *E. coli* had the most retention as manifested by its smallest peak-valued breakthrough curves, followed by *P. aeruginosa*, and *P. fluorescens* (Figure 11). After lipopolysaccharide extraction, all the strains had greater retention as compared to original strains, which was manifested by changes in bacterial breakthrough curves. The enhancement of

bacterial retention in the media was mostly pronounced for *P. fluorescens* and least pronounced for *E. coli*.

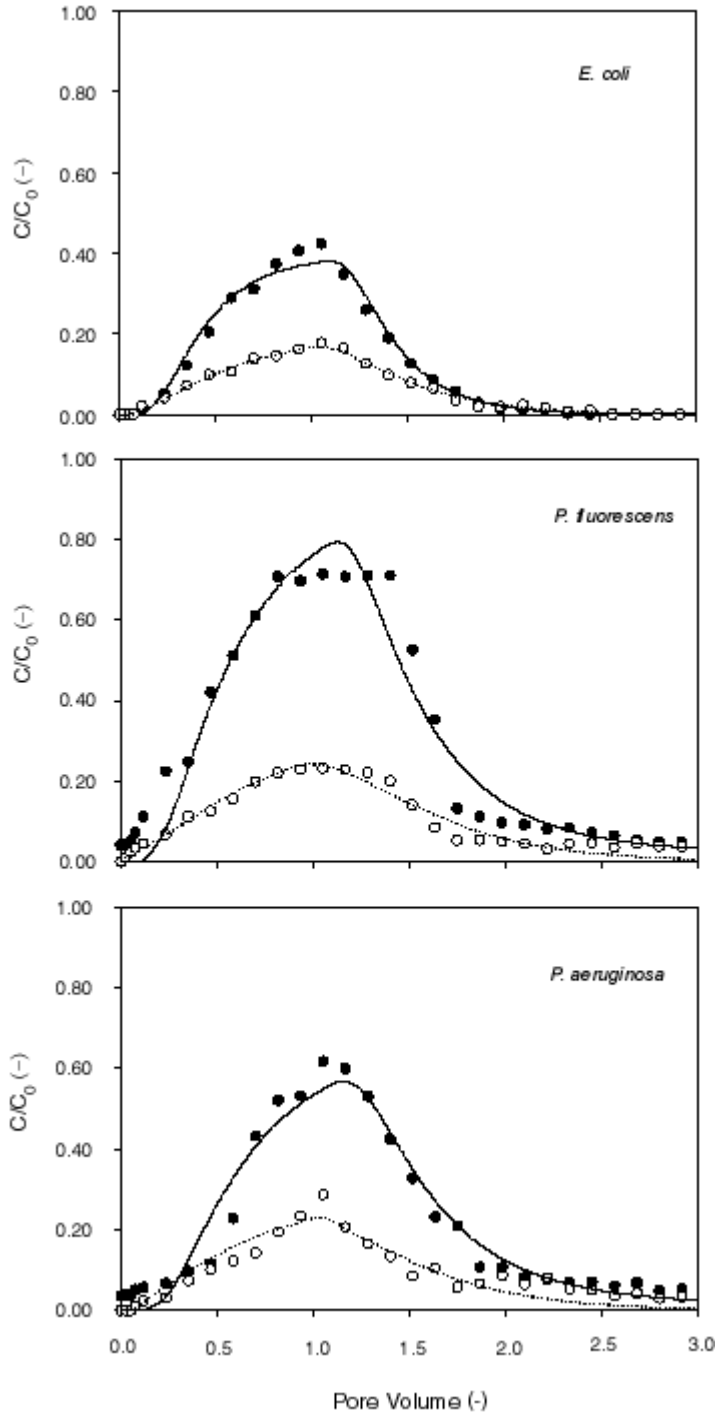

Figure 11. Bacterial Breakthrough Curves (Symbols) and Model Simulations (Lines)

Bacterial breakthrough curves were successfully described by the equilibrium-kinetic two-region concept model (Figures 11). The two-site model provided better descriptions of bacterial transport to account for the complications arising from the potential of bacteria to react with different components of the media matrices. It should be noted that kinetically controlled bacterial adsorption dominates over equilibrium adsorption, which was evidenced by the fact that the simulated f, the fraction of adsorption sites that equilibrate with the bacteria was around 0.2. It was hypothesized that bacterial deposition occurred in the kinetic adsorption region only and was limited by mass transfer between the equilibrium region and the kinetic region. The simulated deposition coefficients were 1.22 min^{-1} for *E. coli*, 0.002 min^{-1} for *P. fluorescens*, and 0.379 min^{-1} for *P. aeruginosa* (Table 5). After lipopolysaccharide extraction, the deposition coefficient values increased to 2.30 for *E. coli*, 1.58 for *P. fluorescens*, and 1.66 for *P. aeruginosa*. Among these three bacterial strains, the increase was the most pronounced for *P. fluoresens* (99%) and the least for *E. coli* (47%). There is a general trend of increase of K_d, the partitioning coefficient of bacteria to the equilibrium adsorption sites after lipopolysaccharide extraction. Before lipopolysaccharide extraction, *E. coli* had the largest K_d of 0.118 cm^3/g, *P. aeruginosa* the least of 0.041 cm^3/g, and *P. fluorescens* in between of 0.104 cm^3/g. After lipopolysaccharide extraction, K_d increased dramatically for *P. aeruginosa* and moderately for *E. coli* and *P. fluorescens*. There is also a general trend that the mass transfer coefficient increased after lipopolysaccharide extraction. The increase was more pronounced for *E. coli* (from 0.0006 min^{-1} to 0.038 min^{-1}) and *P. aeruginosa* (from 0.001 min^{-1} to 0.038 min^{-1}) than *P. fluorescens* (from 0.001 min^{-1} to 0.006 min^{-1}).

Table 5. Tow-region Model Parameters of Bacterial Transport

	α (min^{-1})	K_d (cm^3/g)	$\mu_{s,k}$ (min^{-1})
E. coli	0.0006	0.118	1.22
Treated *E.coli*	0.038	0.385	2.30
P. fluorescens	0.004	0.104	0.002
Treated *P. fluorescens*	0.006	0.202	1.58
P. aeruginosa	0.001	0.041	0.379

Treated *P. aeruginosa*	0.038	1.175	1.66

3.3.3 Bacterial Interactions with the Porous Media

The underlying principles behind bacterial retention in the porous media resulted from bacterial interactions with the porous media. Electrostatic interactions have been demonstrated to be the dominating force in controlling bacterial transport in the porous media (8, 9, 20). Both *E. coli*, *P. fluorescens*, *P. aeruginosa*, and silica sand were negatively charged as demonstrated by negative ζ potential values (Table 6). Therefore, electrostatic interactions between bacteria and silica sand were repulsive, which served as the barrier to prevent bacteria to get close to the porous media. These repulsive electrostatic interactions can operate in the range of several tens of nanometers. The electrostatic interaction free energy between bacteria and the porous media can be calculated by (31):

$$\Delta G(y)_{132}^{EL} = \pi\varepsilon\varepsilon_0 R[2\psi_{01}\psi_{02}\mathrm{Ln}(\frac{1+e^{-\kappa y}}{1-e^{-\kappa y}}) + (\psi_{01}^2 + \psi_{02}^2)\mathrm{Ln}(1-e^{-2\kappa y})] \quad (4)$$

where ε and ε_0 are the relative dielectric permittivity of water (78.55 for water at 25°C) and permittivity under vacuum (8.854 x 10^{-12} C/V·m) respectively; R is the bacterial radius (m); 1/κ is the Debye-Hückel length that is also an estimation of the effective thickness of the electrical double layer (21); y is the distance between the bacterial surface (sphere) and the media surface (flat plate) measured from the outer edge of the sphere (m); and ψ_{01}, ψ_{02} are potentials at bacterial and media surfaces, which can be calculated by:

$$\psi_0 = \zeta(1 + z/a)\exp(\kappa z) \quad (5)$$

where ζ is the zeta potential measured at the slipping plate (V); z is the distance from the particle (bacterial cell or silica sand grain) surface to the slipping plate (m); and *a* is the radius of the particle. In equation 3, "1", "2", and "3" denote bacteria, porous media, and water, respectively.

Table 6. Bacterial ζ Potential and Maximum Electrostatic Interactions with the Media

	ζ (mV)	ΔG_{132}^{EL} (Max) (kT^*)
E. coli	- 24.5	1217.3

Treated *E.coli*	- 13.8	398.8
P. fluorescens	- 60.3	1703.5
Treated *P. fluorescens*	- 36.0	745.3
P. aeruginosa	- 47.6	1199.4
Treated *P. aeruginosa*	- 44.5	1078.5

*k the Boltzmann constant (1.38048×10^{-23} J/K) and T is the absolute temperature (K). The ζ potential for the porous media is – 65 mV.

The electrostatic interactions between bacteria and the porous media were initiated when the bacteria were around 30 nm away from the porous media. With the decrease of the separation distance between bacteria and the porous media, the repulsive electrostatic interactions increased (Figure 12). The maximum electrostatic interactions occurred when the separation distance between bacteria and the porous media was in the range of the sum of the double layer thickness of the bacteria and the porous media. Once bacteria overcame the barrier, electrostatic interactions between bacteria and the porous media decreased dramatically and consequently, attractive Lifshitz van der Waals interactions would dominate and bacteria would attach to the media. The maximum electrostatic interactions were the actual barrier of bacterial adhesion to media matrices and thus the determinant factor for bacterial deposition in the porous media. Among the three bacterial strains investigated in this research, *P. fluorescens* had the greatest ΔG_{132}^{EL} (Max), the maximum electrostatic interaction free energy of with the porous media of silica sand (1703.5 kT, k is the Boltzmann constant of 1.38048×10^{-23} J/K and T is the absolute temperature). *E. coli* and *P. aeruginosa* had similar ΔG_{132}^{EL} (Max) (1217.3 kT and 1199.4 kT). After lipopolysaccharide extraction, ΔG_{132}^{EL} (Max) decreased to 398.8 kT, 745.3 kT, and 1078.5 kT for *E. coli*, *P. fluorescens*, and *P. aeruginosa*, respectively (Table 2). By plotting deposition coefficient against ΔG_{132}^{EL} (Max), it was found that deposition coefficient linearly increased with the decrease of ΔG_{132}^{EL} (Max), the maximum electrostatic interaction free energy between bacteria and the porous media (Figure 13). This observation was consistent with previous research (3, 33).

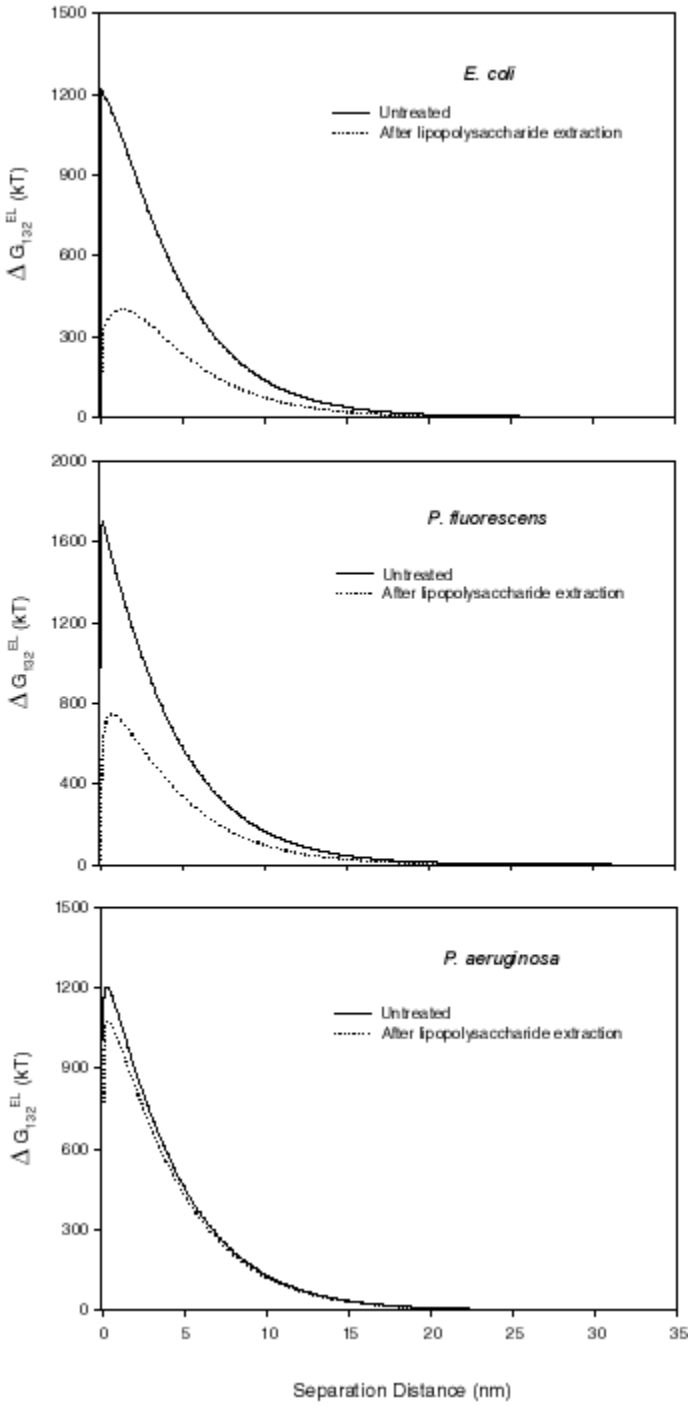

Figure 12. Bacterial Electrostatic Interaction Free Energy as a Function of Separation Distance from the Porous Media

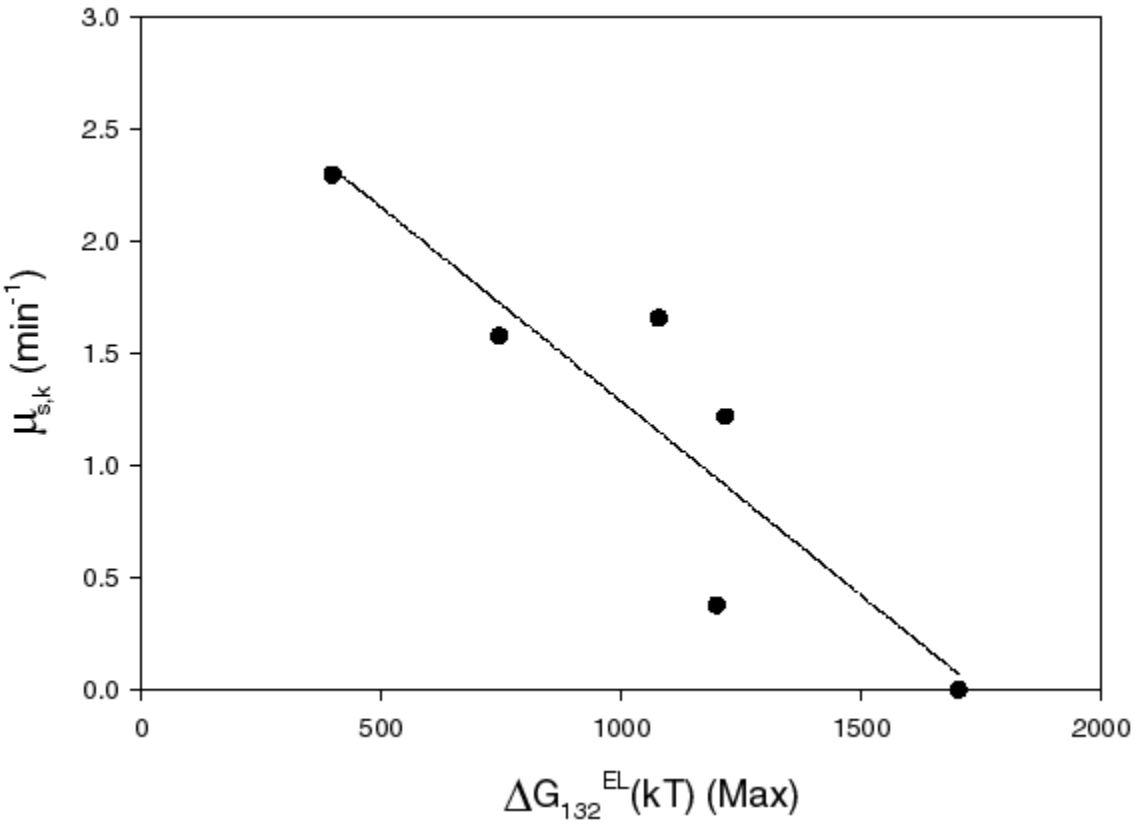

Figure 13. Bacterial Deposition Coefficient as a Function of Maximum Bacterial Electrostatic Interaction Free Energy with the Porous Media

4. Impact of *lux* Gene Insertion on Bacterial Surface Properties

Genetic marker technology has greatly improved our understanding of microbial interactions with the surrounding environment. Currently, developments in genetic marker technology have concentrated on the optimization of the marker system to track, with high sensitivity and reliability, inocula introduced into the environment. *Lux* gene has shown great potential in this area and many different species can now be marked with *lux* gene for a wide range of applications. From this research, it was concluded that *lux* gene insertion impacted bacterial surface thermodynamic properties and transport in the subsurface. After *lux* gene insertion, bacteria displayed stronger interactions with the porous media. Consequently, more bacteria were retained. When genetic marker is used in practice, the impact of gene insertion on bacterial

surface properties and transport cannot be ignored and must be evaluated prior to field applications.

4.1 Material and Method

Bacterial strains used in this research included typical gram-positive bacterial strains of *Lactobacillus casei* (ATCC 11578), *Streptococcus mitis* (ATCC 9456), and *Micrococcus luteus* (ATCC 15176). *L. casei* was cultured in De Man, Rogosa, and Sharpe broth (MRS), *S. mitis* was cultured in Todd Hewitt broth (THB), and *M. luteus* was cultured in nutrient broth. All these three bacterial strains were quantified using Adenosine Triphosphate (ATP) analysis (7).

Plasmid pUCD607 was a kind gift from Dr. Walton at College of St. Scholastica (Duluth, MN), which contains *lux*CDABE. Cells bearing pUCD607 are ampicillin (amp), kanamycin (26), and streptomycin (sp) resistant. Conjugation of pUCD607 into *L. casei*, *S. mitis*, and *M. luteus* used a non-quantitative triparental mating procedure as described below (15). 100 μl of cells from overnight cultures of *E. coli* HB101/pRK2013 (in LB broth), *E. coli* HB101/pUCD607 (in LB broth), and *L. casei*, *S. mitis*, or *M. luteus* were successively overlaid on LB agar plates and incubated at 30^{o}C for 48 hr. Grown cultures were then selected on LB agar plates containing amp (50 μg/ml), km (50 μg/ml), and sp (50 μg/ml). Growth of pUCD607-marked *L. casei*, *S. mitis*, and *M. luteus* was carried out in 250 ml Erlenmeyer flasks containing 100 ml minimal salt media as described below together with appropriate antibiotics. The media had a composition of KH_2PO_4, 160 mg/l; K_2HPO_4, 420 mg/l; Na_2HPO_4, 50 mg/l; NH_4Cl, 40 mg/l; $MgSO_4{\cdot}7H_2O$, 50 mg/l; $CaCl_2$, 50 mg/l; $FeCl_3{\cdot}6H_2O$, 0.5 mg/l; $MnSO_4{\cdot}4H_2O$, 0.05 mg/l; H_3BO_3, 0.1 mg/l; $ZnSO_4{\cdot}7H_2O$, 0.05 mg/l; $(NH4)_6Mo_7O_{24}$, 0.03 mg/l; glucose, 0.2 g/l; and ammonia chloride, 0.06 g/l. The media were adjusted to pH 7.4 with 1 N HCl or 1 N NaOH and sterilized by autoclaving (121^{o}C and 1 atm) for 20 min. Glucose was filter-sterilized and aseptically added to the autoclaved minimal salt media. After inoculated with 1 ml *lux* gene bearing bacteria, the flasks were put on the Gyratory Water Bath Shaker (30^{o}C and 180 rpm) (Model G76, New Brunswick Scientific Co. Inc., Edison, NJ). 1 ml of the samples was withdrawn periodically from the flasks and A_{600} was measured and related to biomass or cell concentration against the standard curves of *E. coli* MM294 grown in LB broth. Another 1 ml of the samples was withdrawn and measured for light emission by a luminometer (TD-20/20, Turner Design, Sunnyvale, CA).

Curves of light emission versus cell concentration were thus generated and used as references for cell concentration quantification.

4.2 Results and Discussion

4.2.1 Bioluminescence and Growth of *lux* Gene Bearing Bacteria

lux genes are expressed by luciferase, which uses oxygen, NADH-reduced flavin mononucleotide ($FMNH_2$), and n-decyl aldehyde as substrates for light production (34). $FMNH_2$ and long-chain fatty aldehyde, oxidized in the presence of oxygen, form an excited but highly stable intermediate that decays slowly and emits light (22). As synthesis of aldehyde for bacterial strains bearing pUCD607 is constitutive, exogenous n-decyl aldehyde is not required (13). On the other hand, the generation of the aldehyde is an ATP- and NADPH-dependent process, which not only increases the metabolic load of the cell but also depends upon the activity of reductases to convert fatty acids into aldehyde substrates (11, 18). Besides, energy must be diverted to different components of electron transport systems for the luminescence production (24). Therefore, metabolic activity of bacteria bearing *lux* genes differs from that of parental bacteria. Variations in bacterial metabolic activity after *lux* gene insertion may result in changes in outer membrane functional proteins and consequently alter the overall outer membrane hydrophobicity, which, in turn, should be demonstrated by changes in bacterial surface properties (23, 29).

Growth of bioluminescent bacterial strains of *L. casei*/pUCD607, *S. mitis*/pUCD607, and *M. luteus*/pUCD607 in minimal salt media showed no lag phase. Light emission during the logarithmic growth stage was most pronounced for *M. luteus*/pUCD607 and least pronounced for *L. casei*/pUCD607 (Figure 14). Light output displayed a linear relationship with respect to biomass concentration during logarithmic growth stage, making it possible to monitor biomass concentration by means of bioluminescence.

4.2.2 Impact of *lux* Gene Insertion on Bacterial Surface Properties

Both *L. casei*, *S. mitis*, and *M. luteus* exhibited a monopolar surface (γ_1^- is at least one order of magnitude greater than γ_1^+) (Table 7) (31). After *lux* gene insertion, both γ_1^- and γ_1^+ decreased

for all the three strains investigated in this study. However, no regular pattern or trend was observed for the surface monopolarity (i.e., γ_1^-/γ_1^+ increased from 17.5 to 18.9 for *L. casei* and from 31.8 to 32.6 for *S. mitis*, while decreased from 28.5 to 26.8 for *M. luteus*). Also, after *lux* gene insertion, γ_1^{LW} decreased while ζ potential increased for all the three strains.

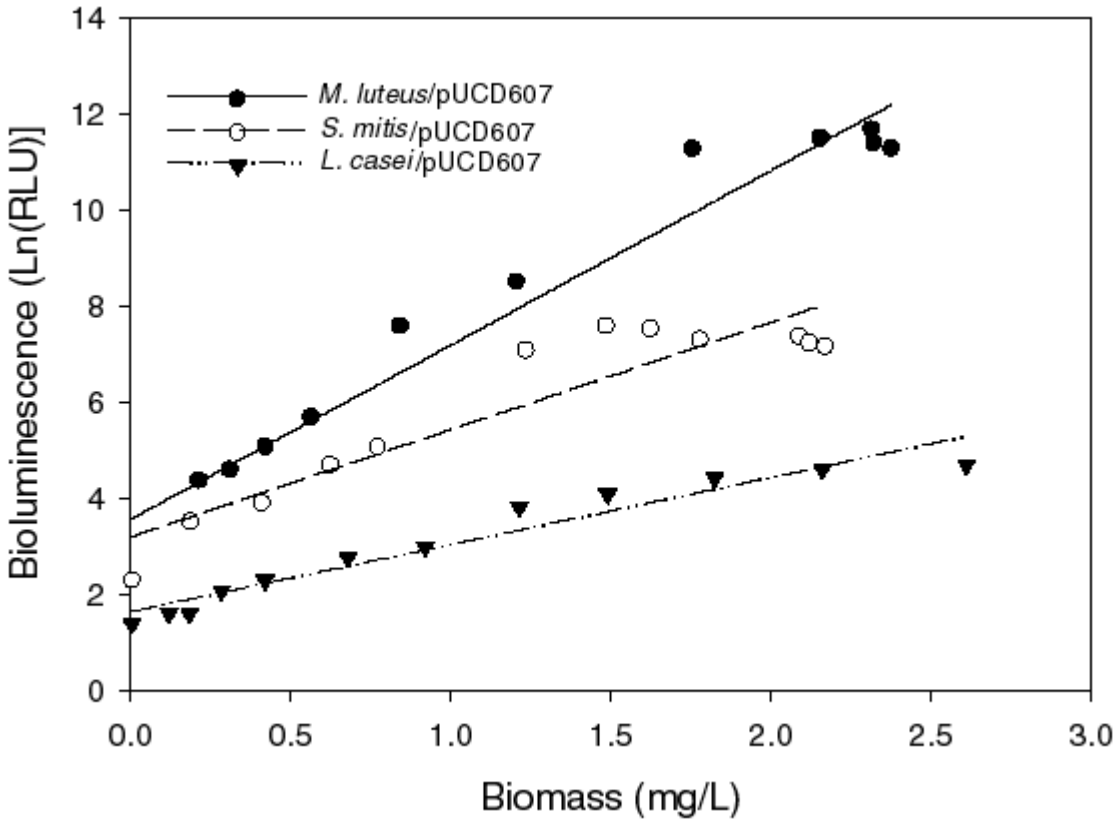

Figure 14. Bioluminescence of *lux*-marked Bacterial Strains

Table 7. Bacterial Surface Thermodynamic Properties

	L. casei	L. casei/ pUCD607	*S. mitis*	S. mitis/ pUCD607	*M. luteus*	M. luteus/ pUCD607
θ^D (°)	22.2 ± 0.3	34.2 ± 0.4	28.8 ± 0.7	36.8 ± 0.6	37.6 ± 0.3	42.0 ± 0.4
θ^F (°)	18.1 ± 0.1	32.5 ± 0.6	28.5 ± 0.6	37.2 ± 0.5	32.6 ± 0.7	40.4 ± 0.5
θ^W (°)	48.6 ± 0.4	55.1 ± 0.7	49.5 ± 0.5	55.0 ± 0.3	49.5 ± 0.2	57.0 ± 0.6

γ^{LW} (mJ/m^2)	47.1	42.4	44.7	41.2	40.8	38.6
γ^{+} (mJ/m^2)	1.18	0.99	0.74	0.65	0.89	0.76
γ^{-} (mJ/m^2)	20.7	18.7	23.5	21.2	25.4	20.4
ζ (mV)	- 24.7 ± 0.8	- 28.1 ± 0.6	- 27.1 ± 0.4	- 32.8 ± 0.7	- 31.6 ± 0.5	- 38.6 ± 0.7

5. Acknowledgements

During this research period, part of the research has been presented at the following workshops and meetings. The sponsorship of USDA-CSREES for this project has been acknowledged (Underline indicates the graduate students working on this project).

1. Chen, G., Impact of *lux* gene insertion on bacterial surface properties and transport, 2008 USDA-CSREES National Water Conference, Sparks, Nevada, February 3-7, 2008.
2. Penagonda Srinivasa Ranga, V. and Chen, G., Impact of lipopolysaccharide extraction on bacterial transport, 60th Annual Meeting of Southeastern Branch of American Society of Microbiology, Auburn, November, 2007.
3. Patil, S. and Chen, G. Bacterial transport as impacted by solution ionic strength, 60th Annual Meeting of Southeastern Branch of American Society of Microbiology, Auburn, November, 2007.

The following papers have been published based on this research and the sponsorship of USDA-CSREES for this project has been acknowledged (Underline indicates the graduate students working on this project and * indicates corresponding author):

1. Penagonda Srinivasa Ranga, V., A. Chan Hilton and G. Chen*, 2008, Lipopolysaccharide Extraction on Bacterial Adhesion and Transport, J. Adhes. Sci. Technol., in press.
2. Chen, G.*, V. Penagonda Srinivasa Ranga, Y. Mao, K. Chen and H. Qiao, 2008, Impact of *lux* gene insertion on bacterial surface properties and transport, Res. Microbiol., 159: 145-151.

6. References

1. **Aldea, M., E. Herrero, M. I. Esteve, and R. Guerrero.** 1980. Surface density of major outer membrane proteins in *Salmonella typhimurium* in different growth conditions. J Gen Microbiol **120:**355-67.
2. **Barnes, R. B., Gore, R.C., Liddel, U. and Williams, V.Z.** 1944. Infrared Spectroscopy, Industrial Applications and Bibliography. Reinhold Publishing Corporation, New York.
3. **Bayoudh, S., A. Othmane, F. Bettaieb, A. Bakhrouf, H. Ben Ouada, and L. Ponsonnet.** 2006. Quantification of the adhesion free energy between bacteria and hydrophobic and hydrophilic substrata. Materials Science & Engineering C-Biomimetic and Supramolecular Systems **26:**300-305.
4. **Boonaert, C. J. P., and P. G. Rouxhet.** 2000. Surface of lactic acid bacteria: Relationships between chemical composition and physicochemical properties. Applied and Environmental Microbiology **66:**2548-2554.
5. **Briandet, R., J. M. Herry, and M. N. Bellon-Fontaine.** 2001. Determination of the van der Waals, electron donor and electron acceptor surface tension components of static Gram-positive microbial biofilms. Colloids and Surfaces B-Biointerfaces **21:**299-310.
6. **Chavant, P., B. Martinie, T. Meylheuc, M. N. Bellon-Fontaine, and M. Hebraud.** 2002. Listeria monocytogenes LO28: Surface physicochemical properties and ability to form biofilms at different temperatures and growth phases. Applied and Environmental Microbiology **68:**728-737.
7. **Chen, G., and K. A. Strevett.** 2001. Impact of surface thermodynamics on bacterial transport. Environmental Microbiology **3:**237-245.
8. **Chen, G., and H. L. Zhu.** 2004. Bacterial deposition in porous medium as impacted by solution chemistry. Research in Microbiology **155:**467-474.
9. **Chen, G. X., and S. L. Walker.** 2007. Role of solution chemistry and ion valence on the adhesion kinetics of groundwater and marine bacteria. Langmuir **23:**7162-7169.
10. **Crook, J., and R. Y. Surampalli.** 1996. Water reclamation and reuse criteria in the US. Water Science and Technology **33:**451-462.
11. **Deweger, L. A., P. Dunbar, W. F. Mahafee, B. J. J. Lugtenberg, and G. S. Sayler.** 1991. Use of bioluminescence markers to detect *Pseudomonas Spp* in the rhizosphere. Applied and Environmental Microbiology **57:**3641-3644.

12. **Drozd, C., and J. Schwartzbrod.** 1996. Hydrophobic and electrostatic cell surface properties of *Cryptosporidium parvum*. Applied and Environmental Microbiology **62:**1227-1232.
13. **Duncan, S., L. A. Glover, K. Killham, and J. I. Prosser.** 1994. Luminescence-based detection of activity of starved and viable but nonculturable bacteria. Applied and Environmental Microbiology **60:**1308-1316.
14. **Flint, S. H., J. D. Brooks, and P. J. Bremer.** 1997. The influence of cell surface properties of thermophilic *streptococci* on attachment to stainless steel. Journal of Applied Microbiology **83:**508-517.
15. **Grant, F. A., J. I. Prosser, K. Killham, and L. A. Glover.** 1992. Luminescence based detection of *Erwinia-Carotovora Subsp Carotovora* in Soil. Soil Biology & Biochemistry **24:**961-967.
16. **Grasso, D., B. F. Smets, K. A. Strevett, B. D. Machinist, C. J. VanOss, R. F. Giese, and W. Wu.** 1996. Impact of physiological state on surface thermodynamics and adhesion of *Pseudomonas aeruginosa*. Environmental Science & Technology **30:**3604-3608.
17. **Hancock, I., and I. Poxton.** 1988. Bacterial Cell Surface Techniques. John Wiley & Sons, New York.
18. **Harkins, M., A. J. R. Porter, and G. I. Paton.** 2004. The role of host organism, transcriptional switches and reporter mechanisms in the performance of Hg-induced biosensors. Journal of Applied Microbiology **97:**1192-1200.
19. **Harvey, R. W., and S. P. Garabedian.** 1991. Use of colloid filtration theory in modeling movement of bacteria through a contaminated sandy aquifer. Environmental Science & Technology **25:**178-185.
20. **Jiang, D., Q. Huang, P. Cai, X. Rong, and W. Chen.** 2007. Adsorption of *Pseudomonas putida* on clay minerals and iron oxide. Colloids and Surfaces B-Biointerfaces **54:**217-221.
21. **Marshall, K. C., Breznak, J. A., Calleja, G. B., Mcfeters, G. A., Rutter P. R.** 1984. Microbial Adhesion and Aggregation. Springer-Verlag, New York.
22. **Meighen, E. A.** 1991. Molecular biology of bacterial bioluminescence. Microbiological Reviews **55:**123-142.

23. **Molin, S., Givskov, M.** 1999. Application of molecular tools for in situ monitoring of bacterial growth activity. Environmental Microbiology **1:**383-391.
24. **Paton, G. I., C. D. Campbell, L. A. Glover, and K. Killham.** 1995. Assessment of bioavailability of heavy metals using *lux* modified constructs of *Pseudomonas fluorescens*. Letters in Applied Microbiology **20:**52-56.
25. **Powelson, D. K., and A. L. Mills.** 1998. Water saturation and surfactant effects on bacterial transport in sand columns. Soil Science **163:**694-704.
26. **Qin, X. S., G. H. Huang, A. Chakma, B. Chen, and G. M. Zeng.** 2007. Simulation-based process optimization for surfactant-enhanced aquifer remediation at heterogeneous DNAPL-contaminated sites. Science of the Total Environment **381:**17-37.
27. **Rosenberg, M.** 1991. Basic and applied aspects of microbial adhesion at the hydrocarbon-water interface. Critical Reviews in Microbiology **18:**159-173.
28. **Sharma, P. K., and K. H. Rao.** 2002. Analysis of different approaches for evaluation of surface energy of microbial cells by contact angle goniometry. Advances in Colloid and Interface Science **98:**341-463.
29. **Singleton, P.** 1997. Bacteria in biology, biotechnology and medicine. John Wiley & Sons, New York.
30. **Smets, B. F., D. Grasso, M. A. Engwall, and B. J. Machinist.** 1999. Surface physicochemical properties of *Pseudomonas fluorescens* and impact on adhesion and transport through porous media. Colloids and Surfaces B-Biointerfaces **14:**121-139.
31. **van Oss, C. J.** 1994. Interfacial Forces in Aqueous Media. Marcel Dekker, New York.
32. **Vangenuchten, M. T., and R. J. Wagenet.** 1989. Two-site/two-region models for pesticide transport and degradation: Theoretical development and analytical Ssolutions. Soil Science Society of America Journal **53:**1303-1310.
33. **Vanloosdrecht, M. C. M., J. Lyklema, W. Norde, and A. J. B. Zehnder.** 1989. Bacterial adhesion: A physicochemical approach. Microbial Ecology **17:**1-15.
34. **Ziegler, M. M., and T. O. Baldwin.** 1981. Biochemistry of bacterial bioluminescence. Current Topics in Bioenergetics **12:**65-113.

7. Appendices

7.1 Abstract of "**Impact of Lipopolysaccharide Extraction on Bacterial Transport**", presented at the 60th Annual Meeting of Southeastern Branch of American Society of Microbiology, Auburn, November, 2007.

7.2 Abstract of "**Bacterial Transport as Impacted by Solution Ionic Strength**", presented at the 60th Annual Meeting of Southeastern Branch of American Society of Microbiology, Auburn, November, 2007.

7.3 Agenda of 2008 USDA-CSREES National Water Conference, Sparks, Nevada, February 3-7, 2008, where "**Impact of *lux* Gene Insertion on Bacterial Surface Properties and Transport**" was presented.

7.4 "**Lipopolysaccharide Extraction on Bacterial Adhesion and Transport**", to be published in J. Adhes. Sci. Technol.

7.5 "**Impact of *lux* Gene Insertion on Bacterial Surface Properties and Transport**", published in Res. Microbiol. (Vol. 159, page 145-151).